

Research papers

Hydrological network and classification of lakes on the Third Pole



Yang Gao^{a,b,*}, Weicai Wang^{a,b}, Tandong Yao^{a,b}, Ning Lu^{c,d}, Anxin Lu^e

^a Key Laboratory of Tibetan Environment Changes and Land Surface Processes, Institute of Tibetan Plateau Research, Chinese Academy of Sciences, Beijing 100101, China

^b CAS Center for Excellence in Tibetan Plateau Earth Sciences, Beijing 100101, China

^c State Key Laboratory of Resources and Environmental Information System, Institute of Geographic Sciences and Natural Resources Research, Chinese Academy of Sciences, Beijing 100101, China

^d Jiangsu Center for Collaborative Innovation in Geographical Information Resource Development and Application, Nanjing 210023, China

^e Institute of Remote Sensing and Digital Earth, Chinese Academy of Sciences, Beijing 100094, China

ARTICLE INFO

This manuscript was handled by Marco borga, Editor-in-Chief, with the assistance of Marco Toffolon, Associate Editor

Keywords:

Lake hydrological network

Lake classification

Third pole

ABSTRACT

The intensity and form of changes in closed lakes, upstream lakes and outflow lakes on the Third Pole (TP) differ based on their drainage mode. Researchers' insufficient understanding of the hydrological networks associated with lakes hampers studies of the relationship between lakes and climate. In this study, we establish a comprehensive hydrological network for each lake ($> 1 \text{ km}^2$) on the TP using 106 Landsat images, 236 Chinese topographic maps, and SRTM DEM. Three-hundred-ninety-seven closed lakes, 488 upstream lakes and 317 outflow lakes totaling $3,5498.49 \text{ km}^2$, $7,378.82 \text{ km}^2$, and $3,382.29 \text{ km}^2$, respectively, were identified on the TP using 2010 data. Two-hundred-thirty-four closed lakes were found to not be linked to upstream lakes. The remaining 163 closed lakes were connected to and fed by the 488 upstream lakes. The object-oriented analyses within this study indicated that more rapid changes occurred in the surface extent of closed lakes than in upstream lakes or outflow lakes on the TP from 1970 s to 2010. Furthermore, the water volume of the examined closed lakes was almost nine times greater than that of the upstream lakes from 2003 to 2009. All the examined closed lakes exhibited an obvious water volume change compared to the corresponding upstream lakes in the same basin. Furthermore, two case studies illustrate that the annual and seasonal dynamics associated with the changes in closed lakes may reflect climate change patterns, while the upstream lake dynamics may be more controlled by the lakeshore terrain and drainage characteristics. The lake inventory and hydrological network catalogued in this study provide a basis for developing a better understanding of lake response to climate change on the TP.

1. Introduction

The Third Pole (TP), which includes the Tibetan Plateau and its surroundings, is referred to as the “Asian water tower” because it stores a large amount of water in different forms (Qiu, 2008; Immerzeel et al., 2010; Yao et al., 2012a). > 1000 lakes ($> 1 \text{ km}^2$) with a total area $> 4 \times 10^4 \text{ km}^2$ have been recorded on the TP from the 1970s to 2010 (Wang et al., 1998; Ma et al., 2010; Zhang et al., 2014). These alpine lakes have been used as laboratories to explore the hydrologic process, evaluate water resources and understand climate change (Yang et al., 2011). During the past four decades, most lakes on the TP shrank between the 1970s and 1990, followed by a slight and then greater expansion in the 1990s and 2000s, respectively (Zhang et al., 2014). Regionally, most lakes in the southern TP shrank while those in the central TP expanded greatly (Song et al., 2013). These changes in lake surface extent are primarily caused by trade-offs between surface runoff

from precipitation, on-lake precipitation, glacier meltwater runoff (glacier-fed lake) and lake water evaporation (Zhang et al., 2017). Case studies and more general research indicate that increased precipitation/decreased evaporation and accelerated glacier retreats identified in the region are the primary factors driving recent lake expansions and mass gains (Lei et al., 2014; Song et al., 2014; Zhu et al., 2010; Zhang et al., 2011), yet the primary drives forces and climate-driven mechanisms of lake variations still remain debated.

Few studies have analysed the impact of a river's structure, whether a lake is closed or runs off to other lakes or rivers, on its relationship to climate patterns (Phan et al., 2013). Closed lakes have an inlet but no outlet. Water in a closed lake does not leave the basin as surface runoff. Those with an inlet and outlet are defined as upstream lake when the runoff flows into a closed lake and as outflow lakes when the runoff connects to a river or eventually flows into the ocean. These three types of lakes have different drainage modes, so the effect of climate change

* Corresponding author at: No. 16 Lincui Road, Chaoyang District, Beijing 100101, China.
E-mail address: yanggao@itpcas.ac.cn (Y. Gao).

on their intensity and forms may differ. It's necessary to distinguish between these lakes and consider them separately in lake-climate researches. However, the comprehensive hydrological network of lakes on the TP has not been delineated, and an understanding of this network's characteristic is lacking. The primary aims of this work are to: identify the hydrological networks associated with each lake on the TP, including the catchments, streams, runoff inputs into lakes, and how lakes are connected to one another or to rivers to classify the lakes as closed, upstream or outflow lakes; explore the different dynamic between these lake types. The rest of the paper is organized as follows: sections 2 and 3 describe the study area, data and methods used in this paper. Section 4 details the results of the hydrological network analysis and classification of lakes on the TP, as well as provides a comparison and evaluation of closed lake, upstream lake and outflow lake dynamics. Section 5 concludes the paper by summarizing the major results of this study.

2. Study area

The TP covers an area over 5,000,000 km² with an average elevation over 4000 m, stretching counterclockwise from the Hindu Kush in the west to the Himalayas in the south, to the Hengduan Mountains in the east, and to the Qilian and Kunlun Mountains in the north. The climate over the southern part of the TP is primarily controlled by the Indian monsoon in the warm season and the westerlies in the cold season. That over the central to northern parts of the TP is primarily controlled by the westerlies, with limited influence from the east Asian monsoon (Yao et al., 2012b). These two circulation systems, combined with the extensive relief, induce strong temporal and spatial heterogeneity in the TP's climate. Over the past four decades, climate over the TP has changed rapidly. Temperature on the TP has risen 0.3–0.4 °C per decade, which is twice the global warming rate (Liu et al., 2000), and the warming in the northern TP is significantly greater than that in the southern TP. Precipitation on the TP increased significantly by 2.2% per decade (Kang et al., 2010). Over the same period, precipitation in the northern TP increased while that in the southern TP decreased (Yao et al., 2012b).

Fig. 1 illustrates the TP zones (Shi et al., 2005). Firstly, the TP is

divided into internal and external drainage area based on the river dividing principle and the supplying relationship between lakes and rivers. External drainage area are defined as hydrological networks connected to other regions via surface runoff, while internal drainage areas are independent hydrological networks. External drainage areas are then subdivided into nine zones including AmuDarya, Inner East Asia, Yellow R. (River), Yangtze R., Mekong R., Salween R., Brahmaputra R., Ganges, and Indus R.. Regional difference in climate and geomorphology are used to subdivide internal drainage areas into seven zones (yellow background color in Fig. 1) including the Qinghai L. (Lake) zone, Ayakku L. zone, DogaiCoring L. zone, BangongCo zone, YibugCaka zone, ZhariNamco zone and SerlingCo zone. Each zone is named after the largest lake therein.

3. Data and methods

3.1. Data

The data used in this study include Landsat images, Chinese Topographic Maps (CTMs), the Map of Glaciers and Lakes on the Tibetan Plateau and adjoining regions (MGLTP), the Shuttle Radar Topography Mission (SRTM) Digital Elevation Model (DEM), and river network and drainage basin data from HydroSHEDS. The Landsat images and CTMs were used to interpret lake boundaries. Maps and image specifications are detailed in Table 1. The MGLTP and CTMs were used to obtain certain lake attributes, including lakes names and type. The SRTM DEM, CTMs and some images were used to delineate the catchment for every lake and construct the hydrological network.

3.1.1. Optical images

The Landsat series MultiSpectral Scanner (MSS), Thematic Mapper (TM) and Enhanced Thematic Mapper plus (ETM+) images have been widely used to map lake boundaries. To reduce the impact of clouds and seasonal variations, the images are selected using the following criteria: 1) all images used were cloud free over the lake boundary; 2) the image acquisition date was from September to November, that is, at the end of the wet season when the lake water budget is relatively stable (Song et al., 2016; Zhang et al., 2017); and 3) the maximum time between

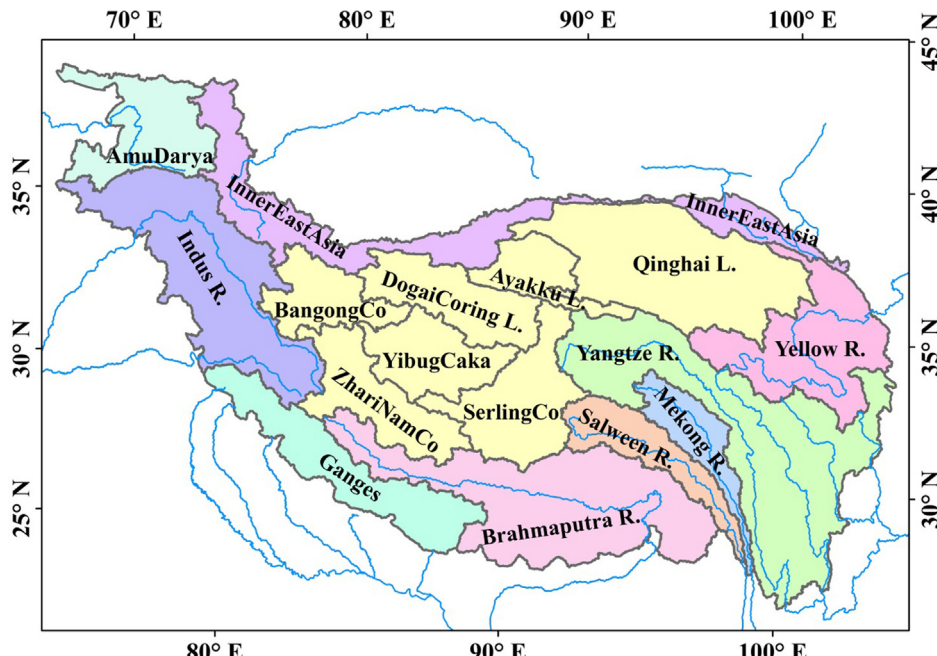


Fig. 1. The zone definition of the Third Pole (The zones with the yellow background belong to the internal drainage area and the others belong to the external drainage area).

Table 1
The maps and images used for identifying the lake boundary.

Decade	Source	Year	Quantity	Utilization
1970s	Chinese topographic maps	1968	20	Lake boundary identification in 1970s based on Chinese topographic maps
		1969	5	
		1970	85	
		1971	63	
		1972	6	
		1973	3	
		1974	18	
		1980	36	
		1972	15	Reference data for lake boundary identification in 1970s
		1973	6	
2010	Landsat MSS	1974	1	
		1975	2	
		1976	40	
		1977	16	
		2009	3/3	Lake boundary identification in 2010 over the Third Pole
		2010	5/92	
		2011	3/0	
2003	Landsat TM/ ETM +	2002	0/1	Lake boundary identification in 2003 and 2009, especially for the 162 lakes whose water lever change rate has been detected
		2003	25/30	
		2004	2/2	
		2009	50/15	

data points was two years if no data were available in a year. However, the coarse spatial resolution and quality of the Landsat MSS images necessitated the use of all available Landsat MSS images from 1972 to 1977. These images were used as reference data in the identification of lake boundaries in the 1970s. In total, 311 Landsat images from the U.S. Geological Survey (USGS) (<http://govis.usgs.gov/>) were used (Table 1). Of these 60 images from 2003 and 65 images from 2009 were used to analyse the change in water volume for 162 typical lakes with available ICESat water level data. To reduce the influence of intra-annual change in a lake's surface extent, all of the images from 2003 and 2009 were obtained between September and November. For the same lake, the difference in the date between photos was within one month. Of the 106 images taken in the 2010s, 90 images were obtained in September to November, which represents 95% lakes. The pre-process procedures include geo-referencing and radiometric correction. Those scenes that have already been systematically calibrated and geo-referenced are used as references for the image-to-image registration of others. The root mean squared errors of the rectifications are controlled within one pixel. Gaps in the Landsat ETM + images are removed using the neighborhood similar pixel interpolator algorithm developed by Chen et al. (2011).

3.1.2. Maps

The CTMs at scale 1:100,000 are based on aerial photography during the period from 1960 to 1980, with spatial resolution of 30 m. They illustrate natural geographical elements such as rivers, lakes and social elements such as villages, roads. Most of this information was verified by field surveying. The geographic coordinate system is the 1954 Beijing Geodetic Coordinate System (BJ54) geoid (datum level is Yellow Sea mean sea level at Qingdao Tidal Observatory in 1956) and the projection is 6-degree Gauss Kruger projection. 236 topographic maps from the National Geomatics Center of China (NGCC) are used (Table 1). Raw geo-reference of these topographic maps is firstly defined and then re-projected into World Geodetic System 1984(WGS84) Universal Transverse Mercator (UTM) projection based on the corresponding Landsat benchmark data.

The MGLTP at scale 1:2,000,000 shows some mountains, rivers, lakes, glaciers as well as the relevant geomorphology, ecology and the transportation network from 70°E to 105°E and from 27°N to 45°N, highlighting the distribution of water resources of glaciers and lakes (Yao et al., 2008). Geo-reference for the map is defined using 55 feature points selected from the benchmark Landsat data and Google earth. A

little offset occurred at the edge of the map due to its large extent. But this offset has no influence on this study since we do not use any geographic information from MGLTP.

3.1.3. SRTM DEM and HydroSHEDS data

The SRTM was launched in February 2000 by the National Geospatial-Intelligence Agency (NGA) and the National Aeronautics and Space Administration (NASA), and it detected the Earth's topography by the single-pass Interferometric Synthetic Aperture Radar technique. The near global (56°S–60°N) SRTM DEM data are with liner vertical absolute height error less than 16 m and relative height error less than 10 m at 90% confidence interval (Farr et al., 2007). The SRTM DEM with cell size of ~87 m and latitude/longitude geographic projection were free available from <http://srtm.csi.cgiar.org/>. The SRTM DEM data from 70°E to 105°E and from 27°N to 45°N are downloaded, mosaicked, and then referenced to the WGS84 horizontal datum. The HydroSHEDS river network (as_riv_15s) and drainage basin (as_bas_15s) with the spatial resolution of ~410 m on TP from the USGS website (<http://hydrosheds.cr.usgs.gov>) are used as a reference data to identify the internal drainage.

3.2. Methods

3.2.1. Making the lake inventory on the TP

A lake vector is an object with an independent position, shape, contour and size. The lake boundaries on the TP in 2003, 2009 and 2010 from Landsat TM and ETM + images have been automatically determined as shown in Fig. 2. The raw digital number (DN) values in the Landsat data were first converted to surface reflectance using the Landsat ecosystem disturbance adaptive processing system (LEDAPS, version 1.2.0; Feng et al., 2013); the surface reflectance provides more appropriate measurements of surface properties than the original DN value or uncorrected radiance and top-of-atmosphere reflectance (Vermote et al., 2002). Next, a two-step automated method was used to identify water pixels by combining the Modified Normalized Difference Water Index (MNDWI) with digital image processing techniques (Jiang et al., 2014). First, the land and water body features were delineated using a deliberately strict threshold. The unmarked pixels may be land or mixed water pixels, which will be classified in the next steps. Second, a watershed segmentation algorithm was used to determine the final lake extent. The algorithm iteratively expands all typical pixels to their neighbor pixels, and the final boundaries between lake and land are determined by the maximum gradient of the MNDWI, which is calculated via the commonly used sobel operator (Meyer, 2012). The segmentation finishes after all of the pixels are marked as lake or land. Next, the extracted lakes rasters are vectorized into lake polygons. The lake boundaries in 1970s and the Landsat ETM + images with gaps are determined by manually visual interpretation based on the enhanced colour images from Landsat MSS and CTMs. Finally, all of the lakes were manually improved and carefully checked one by one by a single expert. In this study, all of the lakes over 1 km² were detected. The water bodies on the major river bed and artificial reservoirs such as Liuyangxia reservoir were excluded from this review. To illustrate the lake evolution, small lakes around a larger lake are identified as independent if they are separated by land.

3.2.2. Establishing the lake hydrological network and classifying the lakes

The lakes' hydrological network includes the catchment of every lake and the main streams. The catchments are used to describe how the runoff from rain, melting snow or ice converges on a lake, and the main streams reveal how lakes connect to other lakes or rivers. This information was derived using three procedures below (Fig. 3). The 2000 SRTM DEM and 1970s CTMs were used to delineate the number of catchment in 2010. Each catchment is surrounded by a geographical barrier, typically a mountain ridge. The uplift rate in the TP was derived from several China Earthquake Administration stations with

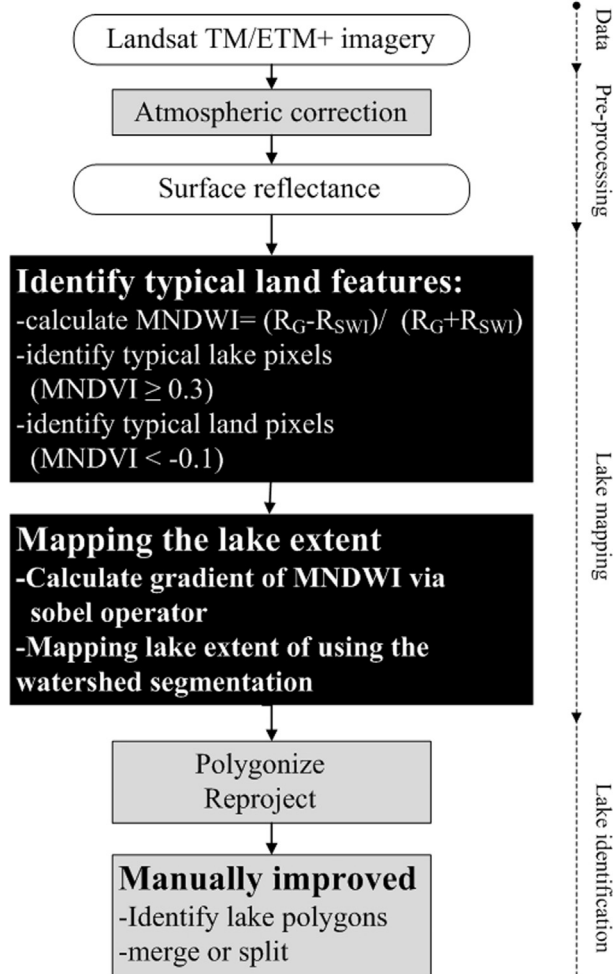


Fig. 2. The method of lake identification (R represents the surface reflectance of the Landsat TM/ETM + data for bands 2 Green (G) and 5 short-wave infrared (SWI)).

continuous GPS measurements. This rate is approximately 0.5 mm/y (Zhang et al., 2013). This small change is unlikely to have caused a change in catchment boundaries between the 1970s and 2010.

1) Calculating a Preliminary Stream Network (PSN) and Drainage Basin (PDB).

Forty-five SRTM DEM tiles over the TP were merged. Automatic delineation, including fill sinks, flow direction, flow accumulation, stream definition, stream segmentation, catchment grid delineation and catchment polygon processing was applied to the merged SRTM DEMs using ArcGIS ArcHydro tools. The threshold for defining streams and the catchments at plateau scale was 4000 ($\sim 32 \text{ km}^2$). Inappropriate search-and-fill process may create some artificial stream networks and basins (Khan et al., 2014); thus, manual quality control and revisions occurred to improve the PSN and PDB.

2) Confirming the drainage links and watershed areas of the closed lakes.

Drainage links and watershed areas were carefully identified and manually revised by a single expert one by one based on rivers and mountain ridges visible on CTMs and Landsat images. The visual inspections were performed at a scale of 1:50,000. First, the lakes, PSN and PDB within every closed HydroSHEDS Drainage Basin (HDB) were separated into independent groups. Within every group, the lake with the lowest elevation from the SRTM DEM and CTMs was determined to be closed within that basin. The stream networks were formatted as polyline vectors and consisted of many oriented river segment routes, running from one node with higher elevation to another with lower elevation. Using each closed lake as a starting point, we upward tracked the PSN from lower elevation to higher elevation until the boundary of the watershed to confirm the drainage links and identify the independent stream network. In some flat area, located mostly in the center of the lake basins, PSN cannot be extracted accurately and only some parallel lines appear. We deleted these lines and re-delineated the river segment roads from the closed lake to the PSN in the light of the rivers in the CTMs, which include most of the main streams. Meanwhile, we found some connected segments were divided into different parts by the HDB. These segments were carefully identified based on the CTMs and Landsat images. If the connection really exists, the connected

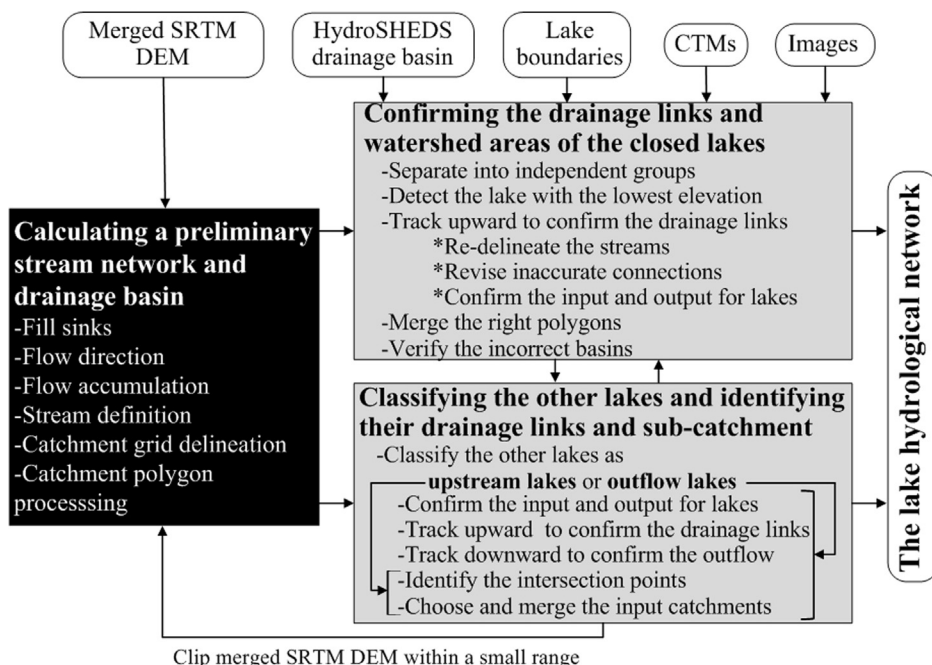


Fig. 3. The method of lake hydrological network establishment.

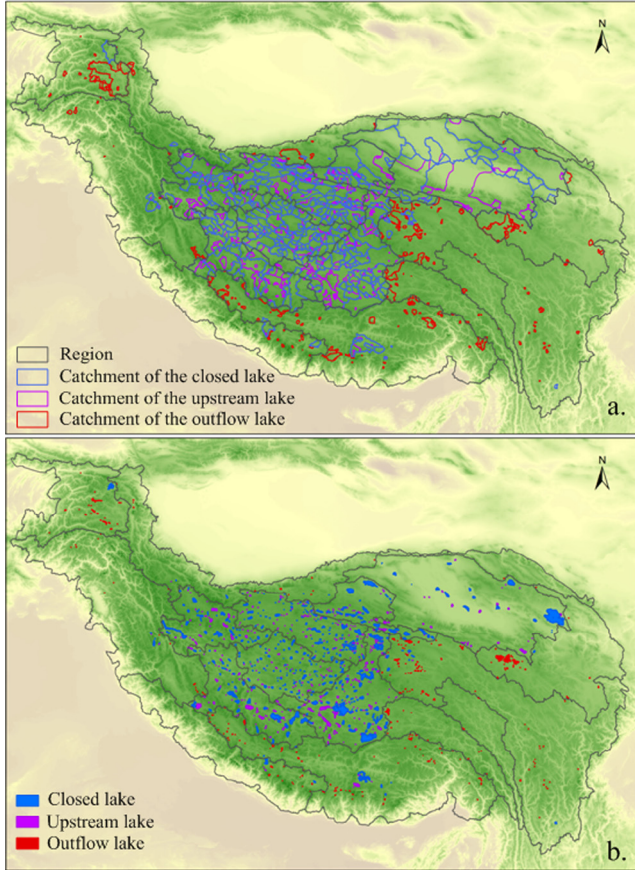


Fig. 4. The catchments (a) and distribution (b) of the closed lake, upstream lake and outflow lake on the third pole in 2010.

neighboring PSNs and PDBs were looked as a new group. The closed lake determination and stream network identification were iterated, and the inaccurate HDB was marked. If not, the false segments were deleted. Especially, the rivers connected with lake were checked to confirm whether they are the input or output according to the elevation difference and the river orientation. After the independent stream network was identified, we merged the PDBs covered the independent stream network into a single closed lake catchment. And then the next independent group was checked until all the groups were done.

3) Classifying the other lakes as upstream or outflow lakes, and identifying their drainage links and sub-catchment. Within every closed lake catchment, all other lakes with the higher elevation than the closed lake were defined as the upstream lakes

(Qiao and Zhu, 2017). This occurred even for lakes where a seasonal river was the only connection between two adjacent lakes. In this case, the lake type was defined based on the seasonal stream's orientation. In the independent stream network, the intersection between every upstream lake and output river was pointed manually. All PDBs found to drain into a given intersection point were merged as sub-catchment of its corresponding upstream lake.

All lakes outside of the closed lakes' catchments were defined as the outflow lakes. Similar with the mentioned method, first the rivers connected with the outflow lake were checked to confirm whether they are the input or output according to the elevation and the river orientation. We began this check from the outflow lake with the lowest elevation because some outflow lakes also have their upstream lakes. Since the runoff from the upstream lakes of the outflow lakes eventually flows into a river and the ocean, we also defined them as the outflow lakes. Using the outflow lake as a starting point, we upward tracked the

PSN to confirm and revise the drainage links. Meanwhile, we downward tracked the PSN to confirm that the output river finally merges into the outflow river. And then the intersection between every outflow lake and output river was pointed manually. All PDBs found to drain into a given intersection point were merged as sub-catchment of its corresponding outflow lake. Here we found some lakes were misclassified as the outflow lakes, because these lakes have no outlet but the HDB dataset were not identified them. Then we redefined them and rebuilt the catchment and stream network according to the above-mentioned method for the closed lake and upstream lake.

56 upstream lakes and 78 outflow lakes were found to have no sub-catchments as they were less than 32 km^2 . To identify sub-catchments within these catchments, we clipped the merged SRTM DEM to a smaller range and ran the hydro process again using a smaller threshold. Catchments for an additional 18 upstream lakes and 7 outflow lakes were delineated manually using the CTMs. These catchments were less than 10 km^2 and were primarily associated with glacier lakes.

3.2.3. Calculating the lake water volume change

Lake water volume change can be modelled by combining time series for a given lake area and water level change rate (Song et al., 2013). Lake water volume change is calculated as:

$$\Delta W = \int_{S_{i-1}}^{S_i} \int_{H_{i-1}}^{H_i} d_S d_H = \frac{(S_i + S_{i-1})}{2} * (H_i - H_{i-1}) \\ = \frac{(S_i + S_{i-1})}{2} * (R_H \times T) \quad (1)$$

where ΔW is the water volume change during the period from i to $i-1$; S_i and S_{i-1} is the lake surface area at i and $i-1$, respectively; and H_i and H_{i-1} represent the water level at i and $i-1$, respectively. R_H is the water level change rate, and T is the time period from i to $i-1$.

The Geoscience Laser Altimeter System (GLAS) on board the Ice, Cloud and Land Elevation Satellite (ICESat) can be used to obtain time series of lake water levels with decimeter accuracy. The available ICESat data for the TP and a linear regression analysis were previously used to develop two published datasets that indicate water level change rates for 117 lakes over 10 km^2 from 2003 to 2009 (Song et al., 2013), as well as those of 154 lakes over 1 km^2 (Phan et al., 2012). In this study, we use these reported water level change rates to calculate the water volume change from 2003 to 2009. The reported lakes can be easily located using the coordinates provided in these datasets.

4. Results and discussion

4.1. The hydrological network and classification of lakes

Fig. 4 shows the catchments and distribution of lakes on the TP in 2010. 1202 lakes with a total area of $46,258.96 \text{ km}^2$ were identified on the TP, including 397 (33%) closed lakes, 488 (41%) upstream lakes and 317 (26%) outflow lakes. These lake types accounted for a total area of $35,498.49 \text{ km}^2$ (77%), $7,378.18 \text{ km}^2$ (16%), and $3,382.29 \text{ km}^2$ (7%), respectively (Table 2). Of the 397 closed lakes, 234 (59%) were not connected to upstream lakes; the remaining 163 (41%) closed lakes were linked to one or more of the 488 upstream lakes. 93% of closed lakes and 96% of upstream lakes were located within the internal drainage area, while all outflow lakes were identified in an external drainage area. Within the external drainage area, the number of lakes associated with the Yangtze R. basin (109 lakes) and Brahmaputra R. basin (103 lakes) exceeded those identified in other regions, and the average area of lakes in the Yellow R. basin (38.2 km^2) was greater than that for any other external drainage area. Within the internal drainage area, the average area of lakes in the Qinghai L. zone was greatest and reached 156.6 km^2 . The average area of lakes in the SelengCo zone, Ayakku L. zone, ZhariNamco zone, and BangongCo zone was 66.0 km^2 , 61.8 km^2 , 60.8 km^2 and 43.2 km^2 , respectively. In the central Dogai-Coring L. zone and YibugCaka zone, the average area of lakes was

Table 2The number and areas of closed lakes, upstream lakes and outflow lakes over 1 km² in different regions of the third pole in 2010.

Region	Lake in 2010		Closed lake				Upstream lake (UL)		Outflow lake	
			Non UL		With UL					
	Num	Area (km ²)	Num	Area (km ²)	Num	Area (km ²)	Num	Area (km ²)	Num	Area (km ²)
InnerEastAsia	19	112.22	4	40.24	1	10.09	1	1.8	13	60.09
Yellow R.	40	1525.97	1	48.29					39	1477.68
Yangtze R.	109	1013.76	5	229.66	3	75.51	7	20.5	94	688.09
Mekong R.	4	38.02							4	38.02
Salween R.	18	256.57							18	256.57
Brahmaputra R.	103	1528.07	6	152.91	2	581.03	5	336.8	90	457.33
Ganges	20	397.13	1	49.49	1	270.07	3	8.81	15	68.76
Indus R.	23	226.58	2	147.37	2	19.71	2	10.99	17	48.51
AmuDarya	28	700.19	1	412.95					27	287.24
Qinghai L.	45	7045.08	8	384.91	7	5760.55	30	899.62		
Ayakku L.	69	4261.09	18	1051.19	17	2928.08	34	281.82		
DogaiCoring L.	197	3604.78	61	683.79	36	2514.47	100	406.52		
BangongCo	81	3502.47	26	673.6	14	2074.59	41	754.28		
YibugCaka	140	2435.45	56	1032.14	31	1161.54	53	241.77		
ZhariNamCo	111	6744.94	15	652.65	21	4353.14	75	1739.15		
SerlingCo	195	12866.64	30	1200.48	28	8990.04	137	2676.12		
TP	1202	46258.96	234	6759.67	163	28738.82	488	7378.18	317	3382.29

18.3 km² and 17.4 km² respectively. These latter values were low given the relatively large number of lakes existed in these two regions (197 and 140 lakes). This indicates that most of the larger lakes are located in the surrounding region while many small lakes are found within the TP.

Fig. 5 shows the differences between the closed catchment identified using the HydroSHEDS data and this dataset, as well as examples of the primary drainage links and sub-catchments within independent basins. Of the 397 closed lakes, 358 lakes had similar boundaries in both the HDB and manually derived dataset, with minor differences in details (see the example in Fig. 5b). These differences were likely due to the spatial resolution of the HDB and the fact that the new drainage basins (blue line) had a higher spatial resolution (90 m) relative to the HDB (~410 m, red line). The other 39 HDBs generally contained four types of errors: a.) The HDBs include some false edges (an example in Fig. 5c, green lines). These were identified by comparing the HDBs to the CTMs and deleting the inaccurate edges. b.) 19 closed lakes and their catchments, including BangongCo, MaindongCo (Fig. 5d), YamzhogYumco, ChemCo, BajiuCo and ChiguCo (Fig. 5e), were not identified using the HDB dataset. We constructed these catchments using the PSN and PDB. c.) Small channels occasionally existed between two nearby lakes; however, the HDB resolution resulted in these lakes being combined into one. For the purposes of this study, these lakes were combined; for example, the DorsoidongCo and MigriggyangzhamCo basins shown in Fig. 5f. and d.) 18 catchments were divided into multiple parts due to the inaccurate classification of segments. For example, in the HDB, an inaccurate segment divides the SerlingCo basin into two; however, we know that this southeastern river is one of three tributaries within the SerlingCo basin (Fig. 5g.).

Two cases representing inaccurate lake linkage identification within the DorsoidongCo & MigriggyangzhamCo (D&M) and SerlingCo basins are shown in Fig. 6. DorsoidongCo and MigriggyangzhamCo are considered independent lakes with their own drainage basins (the red line in Fig. 6a) in the HydroSHEDS data. However, the CTM mapping based on aerial photography from October 1969 (Fig. 6b.), revealed that a seasonal channel existed between these two adjacent lakes, and a seasonal country road passed through the channel. Between the 1970s and 2010, the area of these two lakes reached a minimum in 1996; at that time, this small channel still existed (Fig. 6c.). With the expansion of these two lakes, an obvious channel formed approximately 2002 (Fig. 6d) and the dam that separated these two lakes became more narrow (Fig. 6e). The dam had almost disappeared by 2010 (Fig. 6f). Thus, we identified these two lakes as one lake and merged the PDBs of

these two lakes using the boundary in Fig. 5f. (Black line). Fig. 6g.-l. shows the inaccurate division of SerlingCo based on the HydroSHEDS data. The SerlingCo drainage basin is defined as the red boundary in Figure6g. However, the CTM mapping based on aerial photography from October 1970 (Fig. 6h.) showed that the river Zhagen Zangbu connects UrruCo and SerlingCo. The mean elevations of UrruCo and SerlingCo were 4547 m and 4530 m, respectively, in 1970 and 4553 m and 4539 m, respectively, in 2000. The water in UrruCo flows into SerlingCo through the river Zhagen Zangbu. To confirm that this connection has always existed, four Landsat images from 1976, 1991, 2000 and 2011 were analysed. Then, the UrruCo and SerlingCo PDBs were modified and the boundary of SerlingCo derived (black boundary in Figure5g).

Phan et al. (2013) created drainage links between Tibetan glaciers, lakes and rivers based on a glacier mask, MODIS MOD44W water product and HydroSHEDS river networks. There are two primary differences between Phan's drainage links and the dataset in this study. First, Phan's dataset is based on 891 lakes from the 250 m MODIS MOD44W water product, while the dataset in this study is based on 1197 lakes identified using 30 m Landsat images. Due to the relative higher spatial resolution of the Landsat images, more lakes can be identified. Second, Phan's drainage links were primarily identified based on the HydroSHEDS river network, while the dataset in this study revised the base drainage network using CTMs and multi-period remote sensing images. Zhang et al. (2014) reported that the number and area of lakes over 1 km² on the TP and surroundings were 1236 and 47,366 km² in 2010. The comparison between these two datasets suggests that the difference between the two datasets stems from the definition and interpretation of lakes. First, some water bodies (~257 km²) on the major rivers channels were not counted in the present study, including the Brahmaputra R. and some artificial reservoirs such as Liujiaxia reservoir (~363 km²). Second, islands within lakes, such as the island within the Yamzhog Yumco (~33 km²), were ignored. The most significant difference stemmed from different interpretation of salt lakes (~430 km²). In the present study, we did not include dry lakes or areas that are now dry or only covered by salt.

4.2. Variations in surface extent change between three lake types from 1970s to 2010

The driving mechanism of lake change is a complex combination of multiple climate factors. Meanwhile, the variations in different lakes may be affected by their own hydrological processes. Changes in closed

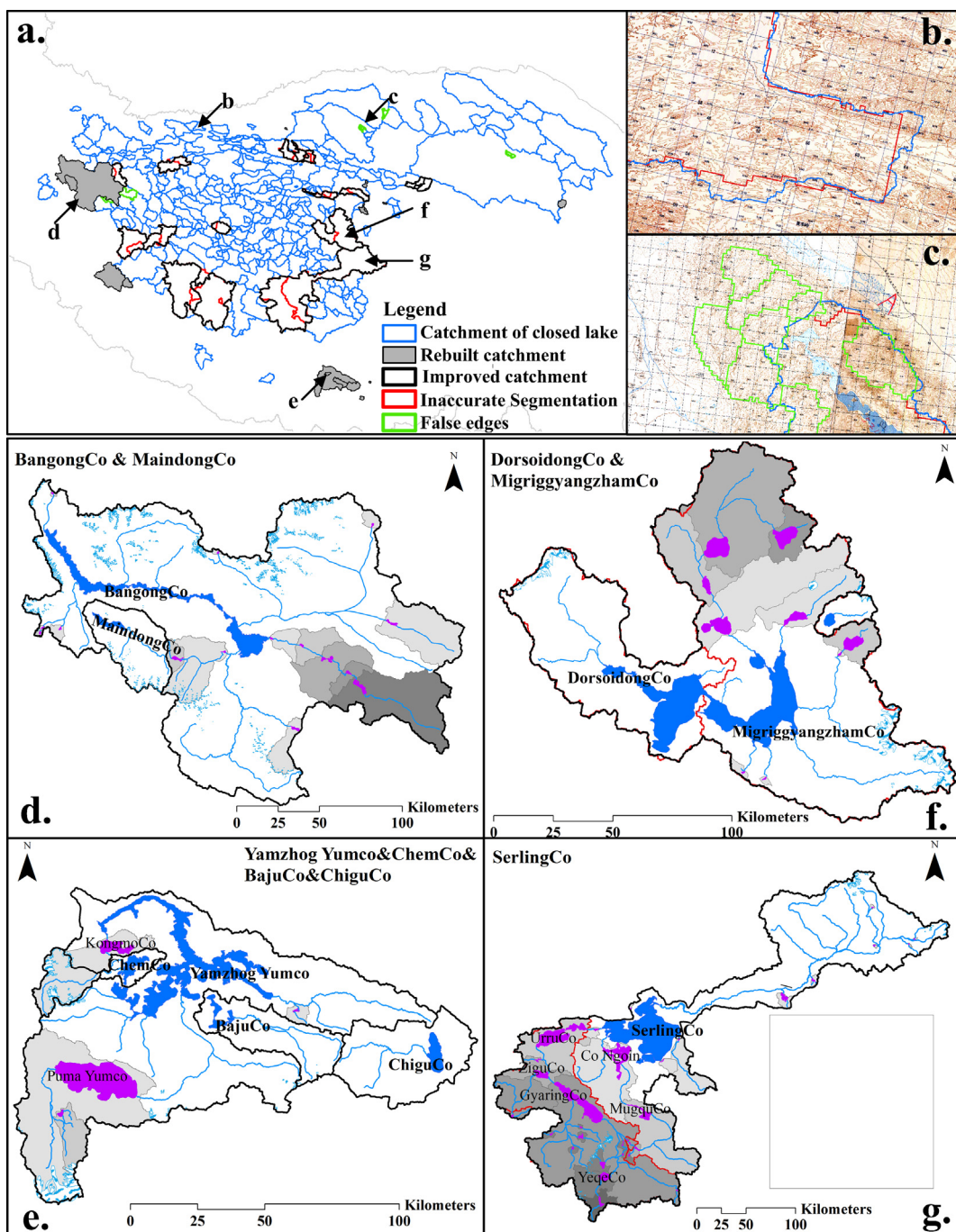


Fig. 5. The differences of the closed catchment between the HydroSHEDS data and this dataset. (a. The types of the differences. b. The comparison of the detailed boundary. c. The example of the false edges from the HydroSHEDS which need to be deleted. d. & e. The examples of the rebuilt catchment. f. The expansion make two independent lakes combine to one. g. The examples of the inaccurate segment boundary and the improved catchment.)

lakes, upstream lakes and outflow lakes from the 1970s to 2010 were summarized in Fig. 7. Most of the closed lakes (91%), upstream lakes (85%) and outflow lakes (75%) expanded during the time frame, increasing by 5,710.6 km², 939.3 km² and 367.8 km², respectively. The number of expanding closed lakes (362) and upstream lakes (413) is comparable, while the increase in area of the closed lakes was 6.1 times that of the upstream lakes and 15.5 times that of the outflow lakes. On the other hand, 35 closed lakes, 70 upstream lakes and 76 outflow lakes shrank during the study period, with decrease decline of −345.9 km², −65.2 km² and −90.5 km², respectively. The larger lakes were generally associated with greater changes in area; however, Fig. 7b indicates that lake size is not the only factor that affects lake area

change. > 54% of expanding closed lakes exhibited an area increase over 5 km², while only 10.2% of expanding upstream lakes and 4% of expanding outflow lakes exhibited increase of that size (Fig. 7b). This indicates that the surface area changes (expanding or shrinking) of closed lakes are more noticeable than those of upstream lakes and outflow lakes.

As mentioned above, 163 closed lakes are supplied by 488 upstream lakes. To further clarify whether changes in the closed lakes occurs more rapidly than those of their corresponding upstream lakes, we divided these lakes into 163 groups. Each group includes one closed lake and their corresponding upstream lakes. From the 1970s to 2010, 16 closed lakes shrank while the other 147 expanded, representing a

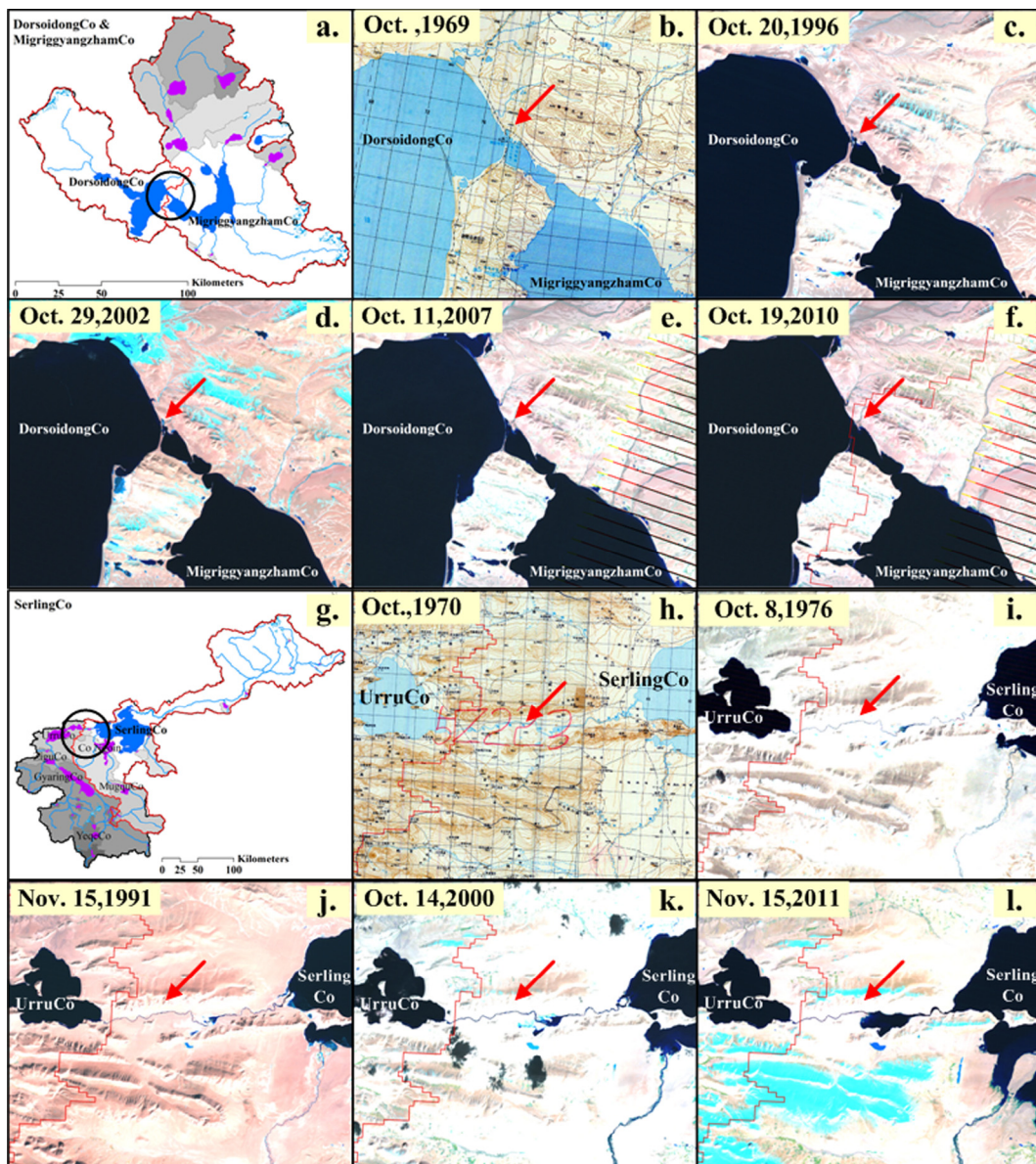


Fig. 6. Two case about the identification of the wrong lake linkage definition in HydroSHEDS data (a. and g. The location of the wrong lake linkage of DorsoidongCo & MigriggyangzhamCo (D&M) and SerlingCo. b., c., d., e. and f. The connection of two lakes respectively in 1969, 1996, 2002, 2007 and 2010; h., i., j., k. and l. The inland river Zhagen Zangbo linked UrruCo and SerlingCo in 1970, 1976, 1991, 2000 and 2011).

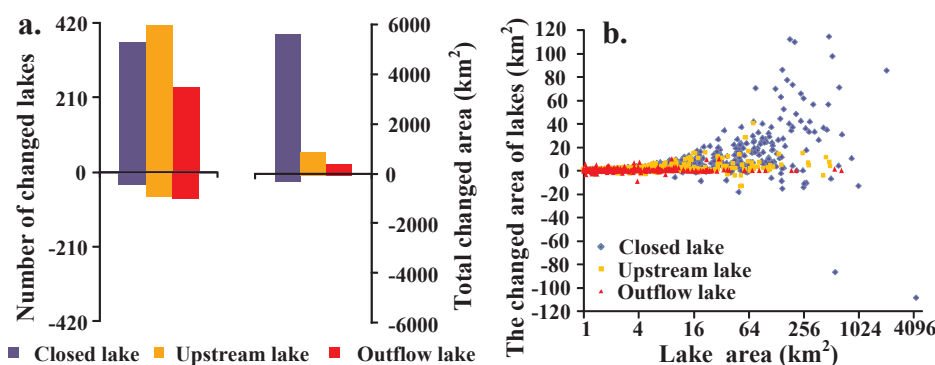


Fig. 7. The change of the closed lakes, upstream lakes and outflow lakes during the period from 1970s to 2010. (a. Number of expansion (positive) or shrinkage (negative) lakes (left plot) and total changed area of expansion (positive) or shrinkage (negative) lakes (right plot); b. The changed area of every lake in 1970s-2010 (To display the majority of lakes change, four lakes with the area increase over 120 km^2 are not shown in Fig. 7b including SerlingCo ($+679.0 \text{ km}^2$), Ayakku L. ($+323.3 \text{ km}^2$), DorsoidongCo ($+150.5 \text{ km}^2$), DogaicoringQangCo ($+149.2 \text{ km}^2$))).

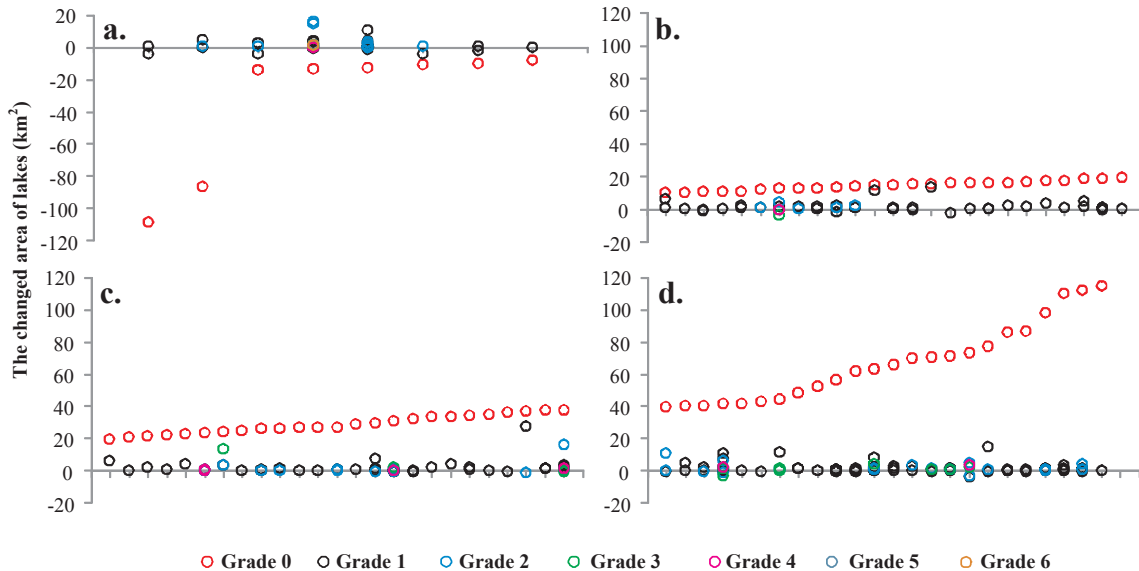


Fig. 8. The changed area of 82 groups of closed lakes and their corresponding upstream lakes during the period from 1970s to 2010. The changed area of the closed lakes are within $-108.2\text{--}8.2\text{ km}^2$ in Fig. 8a, $10.4\text{--}19.5\text{ km}^2$ in Fig. 8b, $19.6\text{--}37.6\text{ km}^2$ in Fig. 8c, $39.9\text{--}114.6\text{ km}^2$ in Fig. 8d. (Grade means the supplying relationship between one closed lake and its upstream lakes. Lake with grade 0 means it is the closed lake; Grade 1 means it is the upstream lake which directly supplies the closed lake; Grade 2 means it is the upstream lake which directly supplies the upstream lake with grade 1, and so on.)

changed area of -108.2 km^2 to 679.0 km^2 . Fig. 8 compares 82 groups of closed lakes and their corresponding upstream lakes. The others are not included due to the relatively smaller changed area of -1.3 km^2 to 9.5 km^2 . Fig. 8a indicates that the decreased in the areas of Qinghai L. and YamzhogYumco were far greater than those of their corresponding upstream lakes, and the other six closed lakes also shrank more than their corresponding upstream lakes. Fig. 8b-d reveal greater expansions of closed lakes relative to their corresponding upstream lakes, with the area increase from 10.4 km^2 to 114.6 km^2 . The top four expanding closed lakes are SerlingCo, Ayakkhu L., DorsoidongCo and DogaicorngQangCo, which increased by 679.0 km^2 , 323.3 km^2 , 150.5 km^2 and 149.2 km^2 , respectively. The change in area for their corresponding upstream lakes was much less than that of the closed lakes, with a changed area of -1.9 km^2 to 11.2 km^2 , 0.5 km^2 to 9.5 km^2 , 0.3 km^2 to 4.9 km^2 , and 0.1 km^2 to 10.8 km^2 , respectively. These comparisons show that no matter the change mode and intensity of the closed lakes, the upstream lakes remained relatively stable.

Some previous studies have compared changes in Lake SerlingCo (SilingCo) to those in CoNgoin (Co'e). The two lakes are within one kilometer of one another and have similar climate conditions, including precipitation, temperature, and evapotranspiration. SerlingCo has expanded dramatically, whereas CoNgoin has remained relatively stable. It is inferred that the critical reason for this difference is that CoNgoin is not supplemented by glacial melt water while SerlingCo is (Meng et al., 2012; Song et al., 2014). However, this inference does not take into account the drainage type of these two lakes. The hydrological network developed in this study indicates that SerlingCo is a closed lake while CoNgoin is an upstream lake that feeds into SerlingCo (Fig. 5g). Thus, water from CoNgoin flows into SerlingCo through the YunzhuZangbo River. The connection between the closed lake and its corresponding upstream lakes likely impacted the dramatic expansion of SerlingCo and the stability of CoNgoin.

4.3. Variations in water level, surface extent and water volume change in three lake types from 2003 to 2009

Two published datasets provide information on the changes in water level of some TP lakes from 2003 to 2009. Of the 154 lakes studied by Phan et al. (2012), 89 were closed lakes, 41 were upstream lakes, 18 were outflow lakes, and six lakes were unidentified. Of the 117 lakes

studied by Song et al. (2013), 87 were closed lakes, 24 were upstream lakes, five were outflow lakes, and one was unidentified. Fig. 9a and d illustrate the water level change rate of these three types of lakes. The average change rate of closed lakes, upstream lakes and outflow lakes is 0.23 m/y (0.25 m/y), 0.10 m/y (0.13 m/y), 0.10 m/y (0.11 m/y), respectively per (Phan et al., 2012; Song et al., 2013). The average change rate of the closed lakes is almost two times greater than that of the upstream lakes. Small differences in the water level change rate of the same lake may exist between these two datasets. For example, SerlingCo has the maximum water level increase of 0.68 m/y vs. 0.63 m/y . This may be the result of the differences in the lakes' elevation data or the noise removal and filtering methods employed (Song et al., 2013). However, these minor differences do not affect the trend comparison. Fig. 9b, c e, and f show the changed area and volume of the examined closed, upstream and outflow lakes from 2003 to 2009, respectively. Most of the closed lakes have an area that fluctuates by approximately 5%, while the upstream lakes and outflow lakes remain relatively stable during this period. The average changed volume of the closed lakes, upstream lakes and outflow lakes is $0.42 \times 10^9\text{ m}^3$ ($0.40 \times 10^9\text{ m}^3$), $0.04 \times 10^9\text{ m}^3$ ($0.06 \times 10^9\text{ m}^3$), $0.07 \times 10^9\text{ m}^3$ ($0.20 \times 10^9\text{ m}^3$), respectively. The changed volume of the closed lakes is almost six to ten times greater than that of the upstream lakes.

Comparing closed lake with their corresponding upstream lakes in the same basin can provide a more direct evidence of these changes. The water level change rate of 10 closed lakes with 20 corresponding upstream lakes and eight closed lakes with 12 corresponding upstream lakes can be obtained from Phan et al. (2012) and Song et al. (2013), respectively. Among these 18 groups, eight groups represent the same closed lakes while some of the corresponding upstream lakes vary. Fig. 10a and d illustrates the water level change rates for these groups and indicate that six and three upstream lakes, respectively, have a greater change rate than their supplied closed lakes. However, all of these upstream lakes remain relatively unchanged in surface extent, while the closed lake undergo greater changes in area and have strong spatial heterogeneity (Fig. 10b and e). Thus, these closed lakes have obviously greater water volume change than their corresponding upstream lakes (Fig. 10c and f).

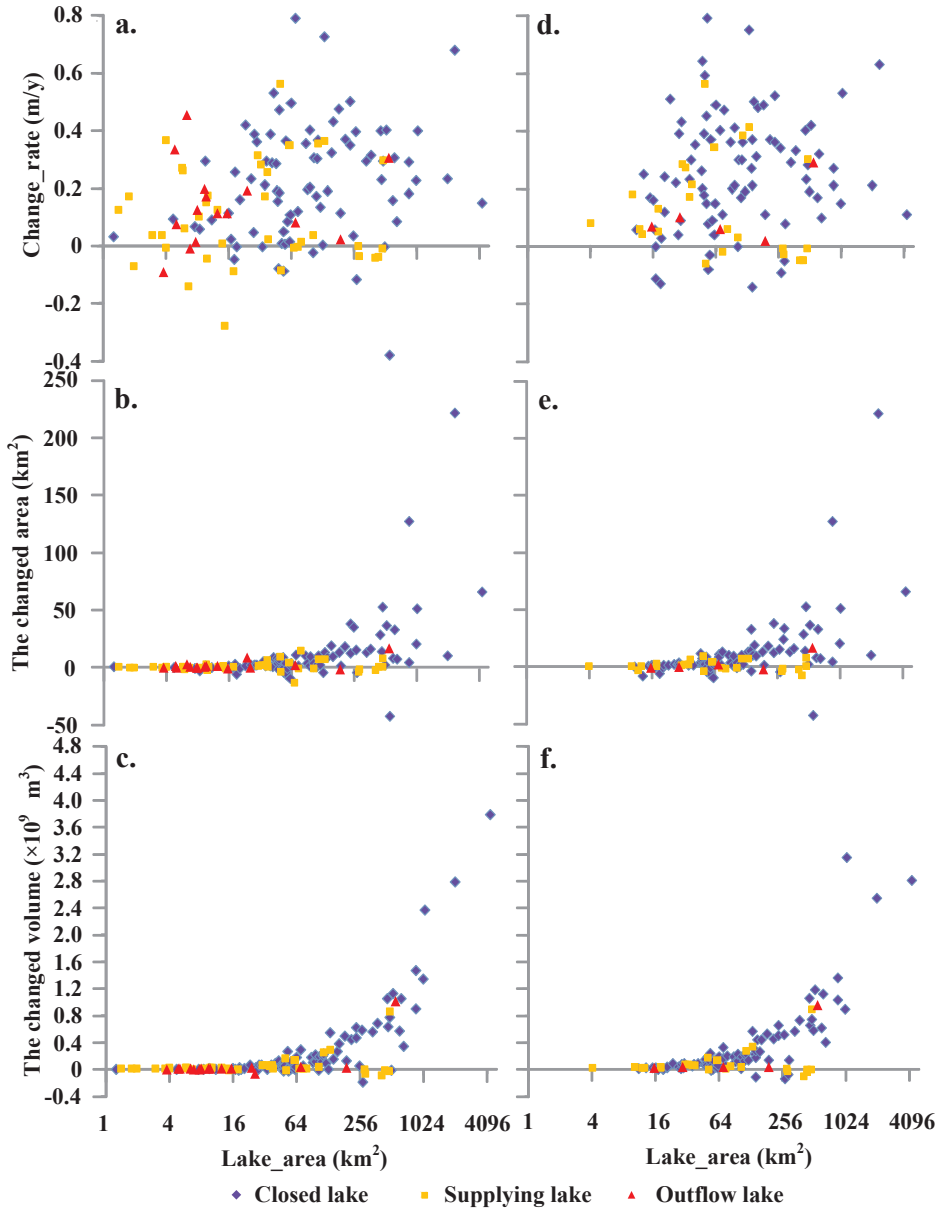


Fig. 9. The comparison of the closed lakes, upstream lakes and outflow lakes in water level, surface extent and volume change during the period from 2003 to 2009 (The values of water level change rate in Fig. 9a. are from Phan et al., 2012, and in Fig. 9d. are from Song et al., 2013; In order to display the vast majority of lakes change in Fig. 9a. and 9c., three closed lakes and one outflow lake whose change rate or volume change over the range are not shown including YamzhogYumCo (-0.38 m/y , $-1.33 \times 10^9 \text{ m}^3$), SerlingCo (0.68 m/y , $9.05 \times 10^9 \text{ m}^3$), L2(0.93 m/y , $0.27 \times 10^9 \text{ m}^3$) and DarksumTso (-0.42 m/y , $-0.07 \times 10^9 \text{ m}^3$)); In Fig. 9d. and f., three closed lakes are not shown including YamzhogYumCo (-0.53 m/y , $-1.86 \times 10^9 \text{ m}^3$), SerlingCo (0.63 m/y , $8.39 \times 10^9 \text{ m}^3$) and CedoCaka (0.89 m/y , $0.32 \times 10^9 \text{ m}^3$)).

4.4. Case studies: Seasonal change in closed lake and upstream lake

Two case studies can be used to compare the seasonal change in area for closed lake and their corresponding upstream lakes: MermaCo and AruCo, DorsoidongCo and RumuchenCo. The MermaCo basin (34.22°N , 82.31°E) is located in the northwest of the internal drainage area of the TP and has an area of 159.24 km^2 . There is only one upstream lake in this basin, AruCo, which has an area of 105.42 km^2 (Fig. 11a). From the 1970s to 2010, the area of MermaCo increases by 21.10 km^2 (13.3%) while that of AruCo increased by 0.33 km^2 (0.3%). From 2003 to 2009, the water level, area and volume change of MermaCo and AruCo were 0.48 m/y , $1.66 \text{ km}^2/\text{y}$, $0.43 \times 10^9 \text{ m}^3$ and 0.03 m/y , $-0.03 \text{ km}^2/\text{y}$ and $0.02 \times 10^9 \text{ m}^3$, respectively. MermaCo and Aruco both begin to freeze in November. MermaCo melts completely by June of the following year, while AruCo melts by May. The closed lake MermaCo has expanded steadily and exhibits a seasonal increase during the non-frozen period from July to October (Fig. 11b.). The change in non-frozen period accounts for 30%-80% of the change throughout the year. Meanwhile, the upstream lake Aruco exhibits almost no seasonal and annual fluctuation (Fig. 11c.).

The DorsoidongCo basin is located at 33.43°N , 90.07°E in the east of the internal drainage area of the TP and has an area of 1032.19 km^2 . It has nine upstream lakes; however, only RumuchenCo has a water level change rate available in ICESat. This lake has an area of 33.74 km^2 . From the 1970s to 2010, DorsoidongCo increased by 150.49 km^2 (14.6%) while RumuchenCo increased by 3.18 km^2 (9.4%). From 2003 to 2009, the water level, area and volume change in DorsoidongCo and RumuchenCo was 0.53 m/y , $11.02 \text{ km}^2/\text{y}$, and $3.15 \times 10^9 \text{ m}^3$ and 0.27 m/y , $0.35 \text{ km}^2/\text{y}$, and $0.05 \times 10^9 \text{ m}^3$, respectively. These two lakes both begin to freeze in November and melt in May next year. The closed lake DorsoidongCo has expanded steadily, and there is an apparent seasonal increase during the non-frozen period from June to October, which account for 74%-97% of the change each year (Fig. 11e.). Meanwhile, the inter-annual area change of the upstream lake RumuchenCo exhibited an increasing trend similar to that of DorsoidongCo from 2006 to 2009, although the absolute change was less than 1.5 km^2 . Furthermore, the upstream lake values fluctuates in the non-frozen period but remained stable in the frozen period (Fig. 11f.). The intra-annual changes in RumuchenCo were similar to those identified for DorsoidongCo in 2003, 2007 and 2009. These two

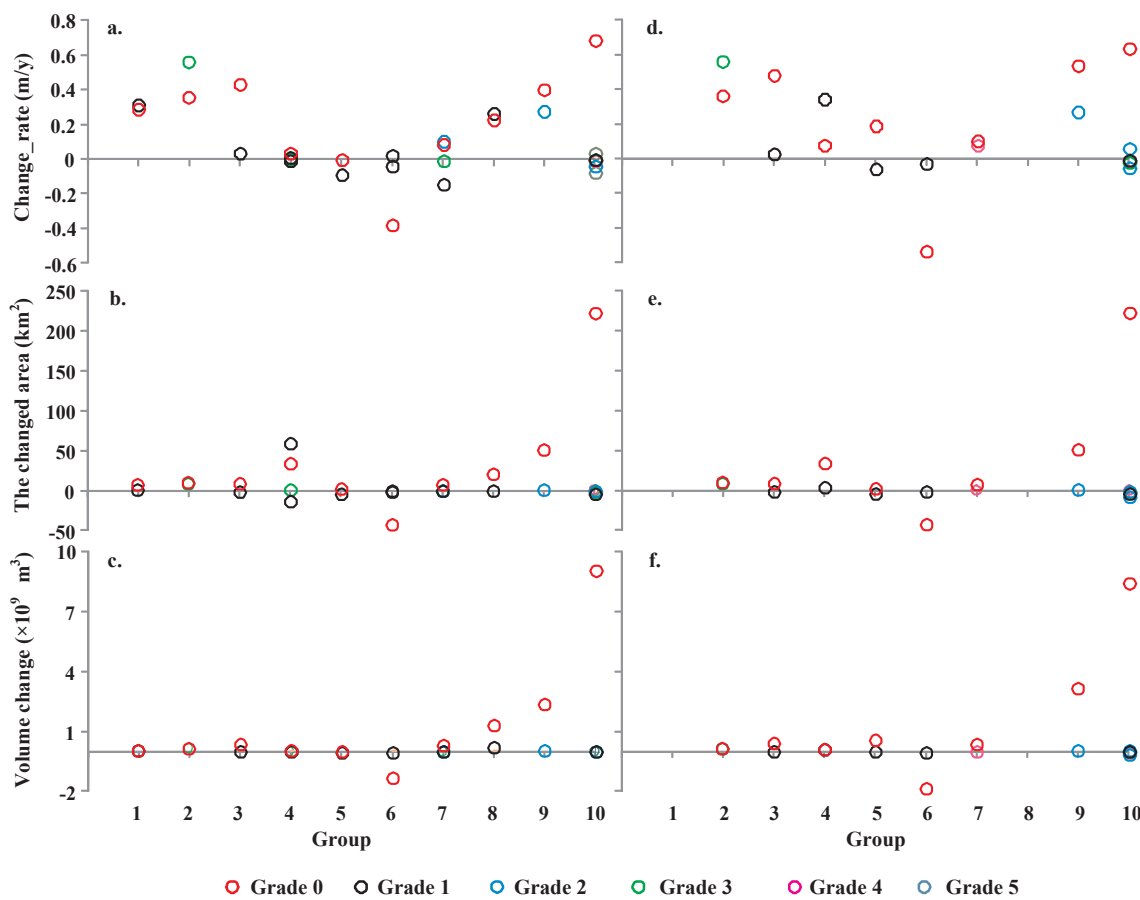


Fig. 10. The water level change rate, changed area and volume of the closed lakes and their corresponding upstream lakes during the period from 2003 to 2009 (The values of water level change rate in Fig. 10a. are from Phan et al., 2012 and Fig. 10c. are from Song et al., 2013; Group 2,3,5,6,7,9,10 are the same closed lakes while some of their corresponding upstream lakes are different.)

case studies indicate that the seasonal and annual change of a closed lake may be linked to climate change. On the other hand, while the seasonal and annual changes in upstream lakes may sometimes reflect climate change, they are more often constrained by the lakeshore terrain and drainage characteristics.

5. Conclusion

Researchers' understanding of hydrological characteristic of lakes on the TP is insufficient, which limits studies interested in the lake-climate relationships. A hydrological network of lakes on the TP was developed to show how runoff converges to a lake and how lake connect to one another or rivers downstream. According to the hydrological network derived in this study, lakes can be classified as closed, upstream or outflow lake. This study indicates that there are 397 closed lakes, 488 upstream lakes and 317 outflow lakes over 1 km² on the TP, with an area of 35,498.49 km², 7,378.18 km², and 3,382.29 km², respectively in 2010. 234 closed lakes are independent and not associated with upstream lakes. The remaining 163 closed lakes are supplied by the 488 upstream lakes. 93% closed lakes and 96% upstream lakes are located in the internal drainage area of the TP, while all of the outflow lakes are located in the external drainage area. Most of the larger lakes are located in the surrounding region while the majority of small lakes are in the interior region in the internal drainage area of the TP.

Closed, upstream and outflow lakes have different drainage modes. The comparison and object-oriented analyses indicate that changes in the surface extent of closed lakes are more apparent than those of upstream lakes and outflow lakes. The increase in area of the closed lakes is 6.1 times that of the upstream lakes and 15.5 times that of the

outflow lakes, although the number of expanding closed lakes and upstream lakes is comparable (362 vs. 413). The closed lake and their corresponding upstream lakes in a given basin show distinct changes, although their hydro-meteorological conditions are similar. The object-oriented analyses further prove that, no matter the mode or intensity of the closed lake changes, the upstream lakes remain relatively stable.

Based on the water level change rate of two published datasets and the lake areas in 2003 and 2009, changes in lake water volume were calculated and analysed. From 2003 to 2009, most of the closed lake areas fluctuated by approximately 5%, while the upstream lakes and outflow lakes remained relatively stable. The water level change rate of the closed lakes is almost two times greater than that of the upstream lakes, while the volume change of the closed lakes is almost nine times greater than that of the upstream lakes. The comparison between the closed lakes and their corresponding upstream lakes further confirms that all the examined closed lakes have an obviously greater volume change than their corresponding upstream lakes, even if some of the closed lakes have less water level change.

Two case studies compare the seasonal area change between closed lakes and their corresponding upstream lakes. MermaCo and AruCo are located in the northwest and DorsoidongCo and RumuchenCo are located in the east of the internal drainage area of the TP. From the 1970 s to 2010, these two closed lake basins exhibited more rapid increases in area than their upstream counterparts. From 2003 to 2009, these two closed lakes exhibited greater water levels, area and water storage changes than their upstream counterparts. These two closed lakes continued to expand steadily and exhibited a seasonal increase during the non-frozen period from June to October. However, the changes exhibited by their associated upstream lakes were different. Aruco

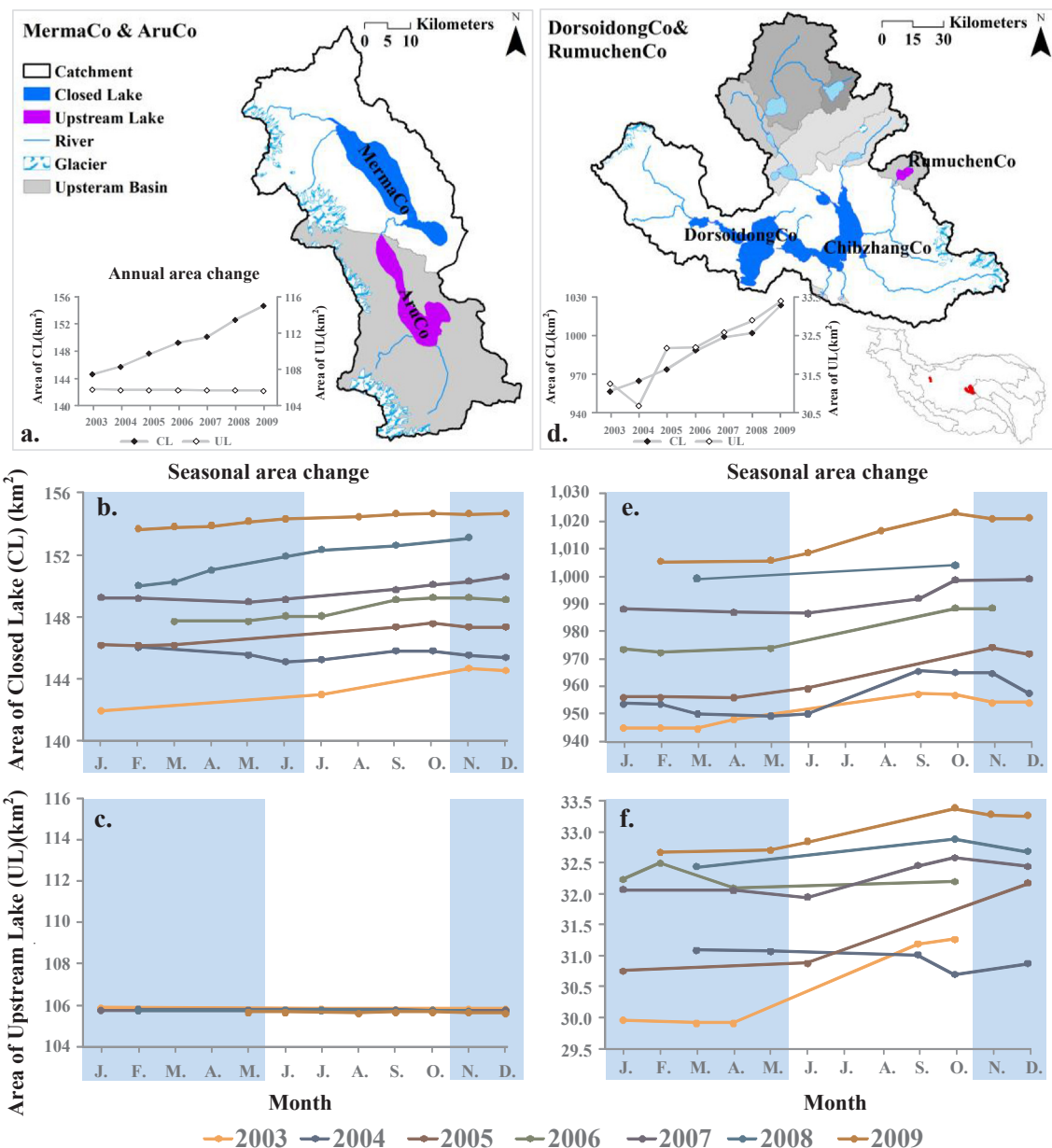


Fig. 11. The seasonal area change comparison between the Closed Lake (CL) and their corresponding Upstream Lake (UL) during the period from 2003 to 2009. (a. and d. are the catchments and drainage network of MermaCo and DorsoidongCo. The line chat in the left bottom show the annual area change comparison of the CL and UL. The map in the right bottom show the locations of these two catchments. b. and c. are the seasonal area change comparison between the MermaCo (CL) and AruCo (UL). e. and f. are that of the DorsoidongCo (CL) and RumuchenCo (UL). The blue shade means the lake-freeze period. And the proportion of the ordinate in Fig. 11b. and 11c. is similar, so does the Fig. 11e. and f.)

exhibited almost no seasonal and annual fluctuation, while RumuchenCo exhibited similar seasonal and annual fluctuation to its closed lake counterpart in some years but not others. Thus, the changes experienced by the closed lakes may be a reflection of climate change while those of the upstream lakes may be limited by the lakeshore terrain and drainage characteristics.

Compared to upstream and outflow lake, closed lakes are the terminal point in a regional water cycle and thus a resultant response to regional climate change. As a result, the change process within closed lakes is much more apparent and significant. To quantify the lake-climate relationship, researchers should investigate whether and how different lakes are connected as well as classify and discuss these lakes separately. The hydrological network and relationship between lakes in this study supports a better understanding of lake responses to climate change on the TP, and provides a basis for additional research in the

climatic, agricultural, environment, water resource management, geomorphological and hydrological fields.

Acknowledgments

This work is supported by the “Key Research Programs in Frontier Sciences” of the Chinese Academy of Sciences (Grant No. QYZDY-SSW-DQC003), the Major Program of National Natural Science Foundation of China (Grant No. 41790432) and the Major Special Project - the China High-Resolution Earth Observation System (Grant No. 30-Y30B12-9003-14/16-01). We would like to thank the U.S. Geological Survey (USGS) for providing Landsat series images, SRTM data, HydroSHEDS river network and drainage basin data, and the National Geomatics Center of China (NGCC) for providing Chinese National topographic maps.

Appendix A. Supplementary data

Supplementary data associated with this article can be found, in the online version, at <http://dx.doi.org/10.1016/j.jhydrol.2018.03.062>.

References

- Chen, J., Zhu, X., Vogelmann, J.E., et al., 2011. A simple and effective method for filling gaps in Landsat ETM1 SLC-off images. *Remote Sens. Environ.* 115 (4), 1053–1064.
- Farr, T.G., Rosen, P.A., Caro, E., et al., 2007. The shuttle radar topography mission. *Rev. Geophys.* 45, RG2004. <http://dx.doi.org/10.1351/dem.2001.0003>.
- Feng, M., Sexton, J.O., Huang, C., et al., 2013. Global surface reflectance products from Landsat: assessment using coincident MODIS observations. *Remote Sens. Environ.* 134, 276–293.
- Immerzeel, W.W., van Beek, L.P., Bierkens, M.F., 2010. Climate change will affect the Asian water towers. *Science* 328 (5984), 1382–1385.
- Jiang, H., Feng, M., Zhu, Y.Q., et al., 2014. An automated method for extracting rivers and lakes from Landsat imagery. *Remote Sens.* 6, 5067–5089.
- Kang, S.C., Xu, Y.W., You, Q.L., et al., 2010. Review of climate and cryospheric change in the Tibetan Plateau. *Environ. Res. Lett.* 5 (1), 015101.
- Khan, A., Richards, K.S., Parker, G.T., et al., 2014. How large is the Upper Indus Basin? The pitfalls of auto-delineation using DEMs. *J. Hydrol.* 509, 442–453.
- Lei, Y.B., Yang, K., Wang, B., et al., 2014. Response of land lake dynamics over the Tibetan Plateau to climate change. *Clim. Change*. <http://dx.doi.org/10.1007/s10584-014-1175-3>.
- Liu, X., Chen, B., 2000. Climatic warming in the Tibetan Plateau during recent decades. *Int. J. Climatol.* 20 (14), 1729–1742.
- Ma, R., Duan, H., Hu, C., et al., 2010. A half-century of changes in China's lakes: global warming or human influence? *Geophys. Res. Lett.* 37, 24106.
- Meng, K., Shi, X., Wang, E., et al., 2012. High-altitude salt lake elevation changes and glacial ablation in Central Tibet, 2000–2010. *Chin. Sci. Bull.* 57 (5), 525–534.
- Meyer, F., 2012. The watershed concept and its use in segmentation: a brief history. In arXiv preprint arXiv:1202.0216.
- Phan, V.H., Lindenbergh, R., Menenti, M., 2012. ICESat derived elevation changes of Tibetan lakes between 2003 and 2009. *Int. J. Appl. Earth Obs. Geoinf.* 17, 12–22.
- Phan, V.H., Lindenbergh, R., Menenti, M., 2013. Geometric dependency of Tibetan lakes on glacial runoff. *Hydrol. Earth Syst. Sci.* 17, 4061–4077.
- Qiao, B., Zhu, L., 2017. Differences and cause analysis of changes in lakes of different supply types in the northwestern Tibetan Plateau. *Hydrol. Process. Hydrol. Process.* 31, 2752–2763.
- Qiu, J., 2008. The third pole. *Nature* 454, 393–396.
- Shi, Y.F., Liu, H.C., Wang, Z.T., et al., 2005. Concise glaciers inventory of China. Shanghai Science Popularization Press, Shanghai (in Chinese).
- Song, C.Q., Huang, B., Ke, L., 2013. Modeling and analysis of lake water storage changes on the Tibetan Plateau using multi-mission satellite data. *Remote Sens. Environ.* 135, 25–35.
- Song, C.Q., Huang, B., Richards, K., et al., 2014. Accelerated lake expansion on the Tibetan Plateau in the 2000s: Induced by glacial melting or other processes? *Water Resour. Res.* 50, 3170–3186.
- Song, C.Q., Sheng, Y.W., 2016. Contrasting evolution patterns between glacier-fed and non-glacier-fed lakes in the Tangula Mountains and climate cause analysis. *Clim. Change* 135, 493–507.
- USGS: Hydrological data and maps based on Shuttle Elevation Derivatives at multiple Scales, available at: <<http://hydrosheds.cr.usgs.gov/index.php>> (access 1212. 2012).
- Vermote, E.F., El Saleous, N.Z., Justice, C.O., 2002. Atmospheric correction of MODIS data in the visible to middle infrared: first results. *Remote Sens. Environ.* 83, 97–111.
- Wang, S.M., Dou, H.S., Chen, K.Z., et al., 1998. China lakes record. Science Press Ltd., Beijing (in Chinese).
- Yao, T.D., Ren, J.W., Xu, B.Q., et al., 2008. Map of glaciers and lakes on the Tibetan Plateau and adjoining regions (1:2000000). Xi'an Cartographic Publishing House.
- Yao, T.D., Thompson, L., Mosbrugger, V., et al., 2012a. Third Pole Environment (TPE). *Environ. Dev.* 3, 52–64.
- Yao, T.D., Thompson, L.G., Yang, W., et al., 2012b. Different glacier status with atmospheric circulations in Tibetan Plateau and surroundings. *Nat. Clim. Change* 2 (9), 663–667.
- Yang, K., Ye, B., Zhou, D., et al., 2011. Response of hydrological cycle to recent climate changes in the Tibetan Plateau. *Clim. Change* 109, 517–534.
- Zhang, Y.S., Yao, T.D., Ma, Y.Z., 2011. Climatic changes have led to significant expansion of endorheic lakes in Xizang (Tibet) since 1995. *Sci. Cold Arid Reg.* 3 (6), 0463–0467. <http://dx.doi.org/10.3724/SP.J.1226.2011.00463>.
- Zhang, G.Q., Yao, T.D., Xie, H.J., et al., 2013. Increased mass over the Tibetan Plateau: From lakes or glaciers? *Geophys. Res. Lett.* 40, 1–6.
- Zhang, G.Q., Yao, T.D., Xie, H.J., et al., 2014. Lakes' state and abundance across the Tibetan Plateau. *Chin. Sci. Bull.* 59 (24), 3010–3021.
- Zhang, G.Q., Yao, T.D., Piao, S.L., et al., 2017. Extensive and drastically different alpine lake changes on Asia's high plateaus during the past four decades. *Geophys. Res. Lett.* 44 (1), 252–260. <http://dx.doi.org/10.1002/2016GL072033>.
- Zhu, L., Xie, M., Wu, Y., 2010. Quantitative analysis of lake area variations and the influence factors from 1971 to 2004 in the Nam Co basin of the Tibetan Plateau. *Chin. Sci. Bull.* 55 (13), 1294–1303.